



# Response of soil respiration to environmental and photosynthetic factors in different subalpine forest-cover types in a loess alpine hilly region

Yuanhang Li<sup>1,2,3</sup> · Sha Lin<sup>1,2,3</sup> · Qi Chen<sup>1,2,3</sup> ·  
Xinyao Ma<sup>4</sup> · Shuaijun Wang<sup>5</sup> · Kangning He<sup>1,2,3</sup>

Received: 28 July 2020 / Accepted: 7 November 2020 / Published online: 1 June 2021  
© Northeast Forestry University 2021

**Abstract** Soil respiration ( $R_s$ ) is important for transporting or fixing carbon dioxide from the atmosphere, and even diminutive variations can profoundly influence the carbon cycle. However, the  $R_s$  dynamics in a loess alpine hilly region with representative sensitivity to climate change and fragile ecology remains poorly understood. This study investigated the correlation and degree of control between  $R_s$  and its photosynthetic and environmental factors in five subalpine forest cover types. We examined the correlations between  $R_s$  and variables temperature ( $T_{10}$ ) and soil moisture content at 10 cm depth ( $W_{10}$ ), net photosynthetic rate

( $P_n$ ) and soil properties to establish multiple models, and the variables were measured for diurnal and monthly variations from September 2018 to August 2019. The results showed that soil physical factors are not the main drivers of  $R_s$  dynamics at the diel scale; however, the trend in the monthly variation in  $R_s$  was consistent with that of  $T_{10}$  and  $P_n$ . Further,  $R_s$  was significantly affected by pH, providing further evidence that coniferous forest leaves contribute to soil acidification, thus reducing  $R_s$ . Significant exponential and linear correlations were established between  $R_s$  and  $T_{10}$  and  $W_{10}$ , respectively, and  $R_s$  was positively correlated with  $P_n$ . Accordingly, we established a two-factor model and a three-factor model, and the correlation coefficients ( $R^2$ ) was improved to different degrees compared with models based only on  $T_{10}$  and  $W_{10}$ . Moreover, temperature sensitivity ( $Q_{10}$ ) was the highest in the secondary forest and lowest in the *Larix principis-rupprechtii* forest. Our findings suggest that the control of  $R_s$  by the environment (moisture and temperature) and photosynthesis, which are interactive or complementary effects, may influence spatial and temporal homeostasis in the region and showed that the models appropriately described the dynamic variation in  $R_s$  and the carbon cycle in different forest covers. In addition, total phosphorus (TP) and total potassium (TK) significantly affected the dynamic changes in  $R_s$ . In summary, interannual and seasonal variations in forest  $R_s$  at multiple scales and the response forces of related ecophysiological factors, especially the interactive driving effects of soil temperature, soil moisture and photosynthesis, were clarified, thus representing an important step in predicting the impact of climate change and formulating forest carbon management policies.

Project funding: This work was supported financially by the National Key Research and Development Plan Projects of China (2017YFC0504604).

The online version is available at <http://www.springerlink.com>

Corresponding editor: Zhu Hong

✉ Kangning He  
hkn@bjfu.edu.cn; li\_voyage@163.com

- <sup>1</sup> School of Soil and Water Conservation, Key Laboratory of State Forestry Administration On Soil and Water Conservation, Beijing Forestry University, Beijing 100083, People's Republic of China
- <sup>2</sup> Beijing Engineering Research Center of Soil and Water Conservation, Beijing Forestry University, Beijing 100083, People's Republic of China
- <sup>3</sup> Engineering Research Center of Forestry Ecological Engineering, Ministry of Education, Beijing Forestry University, Beijing 100083, People's Republic of China
- <sup>4</sup> North China Power Engineering Co., Ltd. of China Power Engineering Consulting Group, Changchun 130021, People's Republic of China
- <sup>5</sup> Power China Huadong Engineering Corporation Limited, Hangzhou 311122, People's Republic of China

**Keywords** Loess alpine hilly region · Soil respiration · Environmental factor · Photosynthesis factor ·  $Q_{10}$  · Two-factor model · Three-factor model

## Introduction

Climate warming from 1880 to 2012 has led to an 0.85 °C increase in the global mean temperatures on land and ocean surfaces (Zhou et al. 2018). Indeed, climate change has huge potential to damage plant growth, water storage, agricultural production and economic activities (Chesney et al. 2017) and exacerbate drought and ecological imbalances. CO<sub>2</sub> also can affect global temperature (Friedlingstein et al. 2014). Soil respiration ( $R_s$ ) is important for transporting or fixing CO<sub>2</sub> in the atmosphere, which is one of the most important carbon fluxes (Wu et al. 2020; Raich et al. 2002). The global soil organic carbon (SOC) pool is approximately twice as large as the OC pool in atmospheric and terrestrial organisms and more than tenfold larger than that caused by human activity (e.g., fuels combustions) (Lal 2008; Hashimoto 2012; Chen et al. 2020). Small variations in  $R_s$  may profoundly influence the carbon cycle and thus affect regional and even global climates through a variety of feedback processes. A potential positive feedback between warmer temperatures and intensive  $R_s$  could eventually accelerate global warming (Vargas et al. 2010a, b).

Therefore, information about  $R_s$  and its controlling environmental factors is of great significance in estimating the concentration of CO<sub>2</sub> in the atmosphere and its impact on global climate change, especially in response to the continuing trend in global warming trend. Monitoring soil temperatures in the field is an effective way to study the response of  $R_s$  to changes in soil temperature (Wertin et al. 2018) and provide a theoretical reference for probing the effects of long-term warming on soil C dynamics (Crowther et al. 2013). The  $R_s$  rates are dominated by soil temperatures ( $T_s$ ) and soil moisture (SWC), which directly affect soil microorganisms and plant root activity and have indirect effects by changing substrate supply and plant growth (Hanson et al. 2000). A moderate temperature increase can accelerate soil humus decomposition and promote autotrophic respiration, thereby facilitating  $R_s$  activity. SWC, the main driver of net primary productivity, can intensely influence the input of C from litter and decompositions of soil organic matter, thereby affecting the output heterotrophic respiration and C output (Moyano et al. 2013). To date, the temperature sensitivity ( $Q_{10}$ ) of  $R_s$  has been shown to decrease with increasing temperature and decreasing SWC (Flanagan and Johnson 2005). Other studies have shown that different forest types differ in the major factors that affect temporal and spatial variation in  $R_s$ , including soil temperature and moisture, root biomass, litter inputs, microbial populations, plant metabolism, other annually or seasonally fluctuating conditions and processes, and even plant phenological patterns (Curiel Yuste et al. 2010; Sheng et al. 2010; Zeng et al. 2014).  $R_s$  is also influenced by soil properties that can change

soil microbial community composition (Landesman et al. 2014), including soil pH, total N, available P, and litter C (Gao et al. 2018; Feng et al. 2014).

Traditionally, the diurnal and seasonal variations in  $R_s$  have been expressed as empirical functions of  $T_s$  or SWC for various ecosystems (Heinemeyer et al. 2012). However, plant photosynthetic activity plays a significant role in regulating and forecasting  $R_s$ , especially in drylands (semiarid and arid areas), which have low levels of microbial activity and organic C in the soil; moreover, litter can lead to rhizosphere respiration becoming the dominant factor in  $R_s$  (Jia et al. 2018) because the source of C for the rhizosphere respiration of plants is provided by photosynthesis. Therefore,  $T_s$  and SWC may not fully represent  $R_s$  across multiple spatial and temporal scales. In addition, diurnal and weekly variation in  $R_s$  may be closely related to canopy photosynthesis, while the correlation between  $R_s$  and canopy photosynthesis (Hölttä 2010) under seasonal and interannual variation needs to be assessed by estimating productivity (Vargas et al. 2010a, b). However, due to the limitations of complex local geographical conditions and other problems, it is difficult to evaluate productivity using an eddy correlation system, a method to explore the annual variation law of  $R_s$  via single leaf photosynthesis (Wertin et al. 2018). In addition, after a large area of near-natural stand transformation occurs, ecosystems with the same stand type will appear as "fragmented" (large-scale pure forest planting area disappears and is replaced by other tree species), which adds to the difficulties and uncertainties in macroscopic analysis of the photosynthetic characteristics of different stand types. Consequently, it may be more accurate to assess the correlation by measuring the combination of single leaf photosynthesis with  $R_s$ .

The study site in the eastern part of the Qinghai-Tibet Plateau is representative of areas that are sensitive to climate change and of fragile, complex ecological environments with unique geographical features (Yao et al. 2005; Fu et al. 2006; Liu and Chen 2000). In recent years, arid and semiarid areas have been identified as potential C sinks (Ardö and Olsson 2003). However, as a major component of the semiarid and arid region, the response to the carbon cycle in various ecosystems under climate change in the Qinghai Tibet Plateau is poorly understood, especially in subalpine forest ecosystems (in contrast to the relatively well-studied  $R_s$  component in alpine, subalpine meadow and permafrost ecosystems) (Ren et al. 2017; Li et al. 2017; Peng et al. 2015). Forest  $R_s$  mainly emerges from the root system, microbial community and soil organic matter metabolism. The habitat provided by different forest stands determines which ecological and biophysiological factors lead to differences in  $R_s$ . Therefore, the annual and seasonal changes in remote sensing for specific types of subalpine forest ecosystems on the

Qinghai-Tibet Plateau, the response to relevant ecological and physiological factors, and the sensitivity to temperature need to be further explored and studied on a multi-spatial scale.

Hence, we established a fitting model between the  $R_s$  and the SWC, the  $T_s$  and combination of SWC and  $T_s$  to illustrate the interaction of temperature and moisture on  $R_s$ . Moreover, we introduce  $P_n$  as the main evaluation factor to establish a three-factor model to more comprehensively assess  $R_s$  regulation and response to various factors in this research area to provide direction and theoretical support for the study of  $R_s$  in typical stands of subalpine forest ecosystems in alpine hilly areas. The objectives were to (1) reveal any multitemporal scale changes in  $R_s$  in different forest covers; (2) test for a correlation between  $R_s$  and  $T_s$ , SWC and combination of  $T_s$  and SWC; (3) evaluate the effect of single leaf photosynthesis on  $R_s$ ; (4) compare the adaptability of different forest covers to warming trends based on  $Q_{10}$ ; and (5) investigate the correlation between  $R_s$  and other ecological environmental factors.

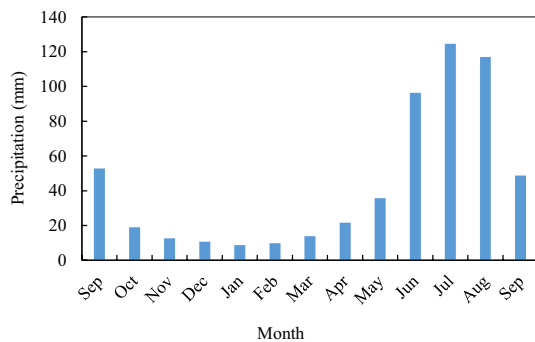


**Fig. 1** Monthly variations in precipitation was presented from September 2018 to September 2019 in study site

## Materials and methods

### Study site

The research was carried out at the several forest reserves in Datong County (37°23'N, 101°51'E) in eastern Qinghai Province, including Tal Gou, Yang Jia Zhai, and An Men Tan. This region is the transition zone between the Qinghai-Tibet Plateau and the Loess Plateau, with an altitude of 2280–4622 m. Typical continental climate predominates in this area, with an annual mean temperature and relative humidity of 4.9 °C and 56%, respectively. The annual mean precipitation and evapotranspiration are 523.3 mm and 1762.8 mm, respectively. April to September (the plant growing season) is the rainy season in which 87% of the rainfall occurs, and the dry season is usually from November to March (Fig. 1). Major afforestation species include *Picea crassifolia* Kom., *Juniperus przewalskii* Kom., *Populus cathayana* Rehd., *Larix principis-rupprechtii* Mayr, *Betula platyphylla* Suk., and *Caragana korshinskii* Kom.

### Experimental plots

Five representative forest covers containing secondary forest ( $S_1$ ), *L. principis-rupprechtii* ( $S_2$ ), *P. crassifolia* ( $S_3$ ), *P. cathayana* ( $S_4$ ) and *B. platyphylla* ( $S_5$ ) plantations were chosen as experimental plots during the spring through early fall of 2018. All slope directions were shady, and slopes did not exceed 20°. The total number of plots (the fixed size was 20×20 m) was 15, which included three replicates (a similar plot was selected according to afforestation data from the local forestry bureau) per forest cover, and each plot was separated by a buffer of at least 20 m. Elevation, slope, tree height, diameter at breast height (DBH), forest age, stand density, canopy density and physical and chemical properties in the topsoil (0–20 cm) were measured for each plot (Tables 1, 2). The main vegetation types of secondary forest were *B. platyphylla*, *L. principis-rupprechtii*, *P. cathayana*, and *P. crassifolia* (not long after replanting, the forest age was 10 years) present at a ratio of 3:3:2:2.

**Table 1** Main stand formation of experimental plots was measured in Loess alpine hilly region

Cover type	Elevation (m a.s.l.)	Slope (°)	Mean tree height (m)	Mean DBH (cm)	Mean forest age (year)	stand density (inds·ha <sup>-1</sup> )	Canopy density(%)
$S_1$	2960.3	14	9.45	12.89	22.4	1800	68
$S_2$	2910.4	13	12.23	15.46	25	2250	80
$S_3$	2919.7	15	13.02	14.25	25	2250	85
$S_4$	2863.6	17	10.34	20.65	30	2000	75
$S_5$	2876.4	18	10.85	14.47	23	2000	70

Notes  $S_1$ ,  $S_2$ – $S_5$  refer to five representative forest covers containing secondary forest ( $S_1$ ), *L. principis-rupprechtii* ( $S_2$ ), *P. crassifolia* ( $S_3$ ), *P. cathayana* ( $S_4$ ) and *B. platyphylla* ( $S_5$ ) plantations

**Table 2** Main topsoil (0–20 cm) physical and chemical properties of experimental plots were measured in Loess alpine hilly region, and the observation of soil respiration was performed simultaneously

Cover type	Bulk density (g·cm <sup>-3</sup> )	pH	SOC (g·kg <sup>-1</sup> )	TN (g·kg <sup>-1</sup> )	TP (g·kg <sup>-1</sup> )	TK (g·kg <sup>-1</sup> )	Soil C:N ratio
S <sub>1</sub>	0.98 ± 0.01c	8.11 ± 0.25a	23.98 ± 1.94a	2.65 ± 0.44a	0.72 ± 0.14a	0.63 ± 0.08a	9.49 ± 0.46b
S <sub>2</sub>	1.08 ± 0.06a	7.53 ± 0.36c	21.61 ± 1.68b	2.13 ± 0.36c	0.44 ± 0.26c	0.36 ± 0.11d	8.07 ± 0.28d
S <sub>3</sub>	1.06 ± 0.04a	7.30 ± 0.23d	18.34 ± 1.45d	1.87 ± 0.42d	0.57 ± 0.13b	0.52 ± 0.16bc	9.81 ± 0.42a
S <sub>4</sub>	1.01 ± 0.03b	7.97 ± 0.35b	19.26 ± 1.52c	2.09 ± 0.35c	0.49 ± 0.12c	0.56 ± 0.15b	9.21 ± 0.97c
S <sub>5</sub>	0.96 ± 0.03c	8.06 ± 0.24ab	17.18 ± 1.76d	2.25 ± 0.57b	0.62 ± 0.08ab	0.48 ± 0.09c	9.60 ± 13.53b

Notes S<sub>1</sub>, S<sub>2</sub>–S<sub>5</sub> refer to five representative forest covers containing secondary forest (S<sub>1</sub>), *L. principis-rupprechtii* (S<sub>2</sub>), *P. crassifolia* (S<sub>3</sub>), *P. cathayana* (S<sub>4</sub>) and *B. platyphylla* (S<sub>5</sub>) plantations

## Experimental design and measurements

### Soil physicochemical properties

Measurements (total two) of all variables were completed in August 2019 according to government standards (Tables 1, 2). Five replicates per plot of undisturbed soil and the soil profile at 0–20 cm depth were collected with cutting rings, placed in separate sealed bags and brought to the laboratory to determine the physical properties of soil. Soil pH can be directly determined with a pH meter (Gao et al. 2018). Soil bulk density was determined using the method of White (1988). Soil samples were dried, ground, and sieved to determine the soil organic carbon (SOC), total nitrogen (TN), total phosphorus (TP), and total potassium (TK) contents as previously described (Clark et al. 1998; Mitchell et al. 1999; Udelhoven et al. 2003; West et al. 1989).

### Soil respiration

From September 2018 to August 2019, in each plot, five PVC soil collars (20 cm in diameter × 10 cm in height) were randomly inserted to a 5 cm depth into the corresponding soil cores, which were extracted with a rubber hammer for  $R_s$  measurement.  $R_s$  was measured using a LI-8100 portable soil CO<sub>2</sub> flux system (LI-Cor Inc., Lincoln, NE, USA) (Xu et al. 2018), soil temperatures at a depth of 10 cm ( $T_{10}$ , °C) were measured with a thermocouple probe (LI-8100–201) connected to the LI-8100 system, and moisture in the 0–10 cm layer ( $W_{10}$ , % vol) near the collar was measured simultaneously with a time-domain reflectometry (TDR) probe (model TDR300, Spectrum Technologies, Plainfield, IL, USA) (Gao et al. 2018). All indicators were observed between 09:00 and 11:00 h at least every 2 weeks because of their accuracy in estimating the daily mean value (Xu and Qi 2001a). In addition, in October 2018 and January, April, and July 2019, we measured diurnal variation every 2 h from 09:00 h to 07:00 h the next day. The final calculated values reflected the average of 5 repeated measurements. Before sampling, the plants in the collars should be carefully removed.

### Photosynthetic variables

$P_n$  was determined for plants around each collar using a LI–COR 6400 photosynthesis system (LI–COR, Lincoln, USA) using randomly selected five fully expanded and representative upper leaves for broad-leaf species *P. cathayana* and *B. platyphylla* and a sprig with numerous leaves for coniferous species *L. principis-rupprechtii* and *P. crassifolia* at the same time as  $R_s$  was measured, including measurement of diurnal variations (daytime: 09:00–19:00 h). After each measurement, the leaf area in the chamber was estimated, and the gas exchange flux was modified accordingly. The leaf area of the plants to be measured was estimated using the leaf area index (LAI), which was determined using fixed points by a canopy analyzer and analyzed by WinSCANOPY2006a. The variation in  $P_n$  in S<sub>1</sub> was obtained by calculating the ratio of total net photosynthetic yield to the total leaf area of the canopy of different tree species in the sample plot.

### Model calculation

To quantify the relationship between  $R_s$ ,  $T_{10}$  and  $W_{10}$ , we established correlation models to analyze and compare the temperature sensitivity in different forest covers. The linear and nonlinear regression models were as follows:

$$R_s = ae^{bT_{10}} \quad (1)$$

$$R_s = aW_{10} + b \quad (2)$$

$$R_s = ae^{bT_{10}} W_{10}^c \quad (3)$$

where  $a$ ,  $b$  and  $c$  are undetermined parameters.  $R_s$  is soil respiration.

$Q_{10}$  was calculated by the following formula:

$$Q_{10} = e^{10b} \quad (4)$$

## Data analyses

Data are represented as the means  $\pm$  standard errors (SE). Means for each variable were analyzed using a one-way ANOVA, and significant differences among the means were tested by Duncan's multiple range test using a significance level of  $\alpha = 0.05$  or  $0.01$  via SPSS 26.0 (IBM, Armonk, NY, USA). Means for several important parameters were tested for correlations using a Pearson correlation analysis. Simple linear regression analyses were used to examine the relationships between relative changes in  $R_s$  and  $Q_{10}$  values, and linear or nonlinear regression was used to evaluate the relationships between  $R_s$  and SOC, TN, TP, TK, soil C: N ratio, and  $P_n$ , which described the effects of biotic and abiotic factors on  $R_s$ . Results were plotted using Origin 2018 software (OriginLab, Massachusetts, USA).

## Results

### Diurnal variations in $R_s$ and $P_n$

Maximum and minimum values for  $R_s$  were measured at 15:00–17:00 and 5:00–7:00, respectively (Fig. 2A).  $R_s$  of broad-leaf species was markedly higher than that of coniferous species during spring, summer, and autumn. Compared with the pure forest ( $S_2$ – $S_5$ ), the mixed secondary forest ( $S_1$ ) had significantly higher values, except in winter ( $p < 0.05$ ). During winter, no dramatic variation was detected in any forest covers ( $p > 0.05$ ).

The diurnal variation in  $T_{10}$  in each stand did not significantly fluctuate, except in April, and the temperature was higher during the day than at night. Moreover, the amplitude of variation was marginal in  $W_{10}$ , with only a certain fluctuation in April and July (Fig. 2B, C). The variation in  $W_{10}$  was remarkable in S4 during summer.

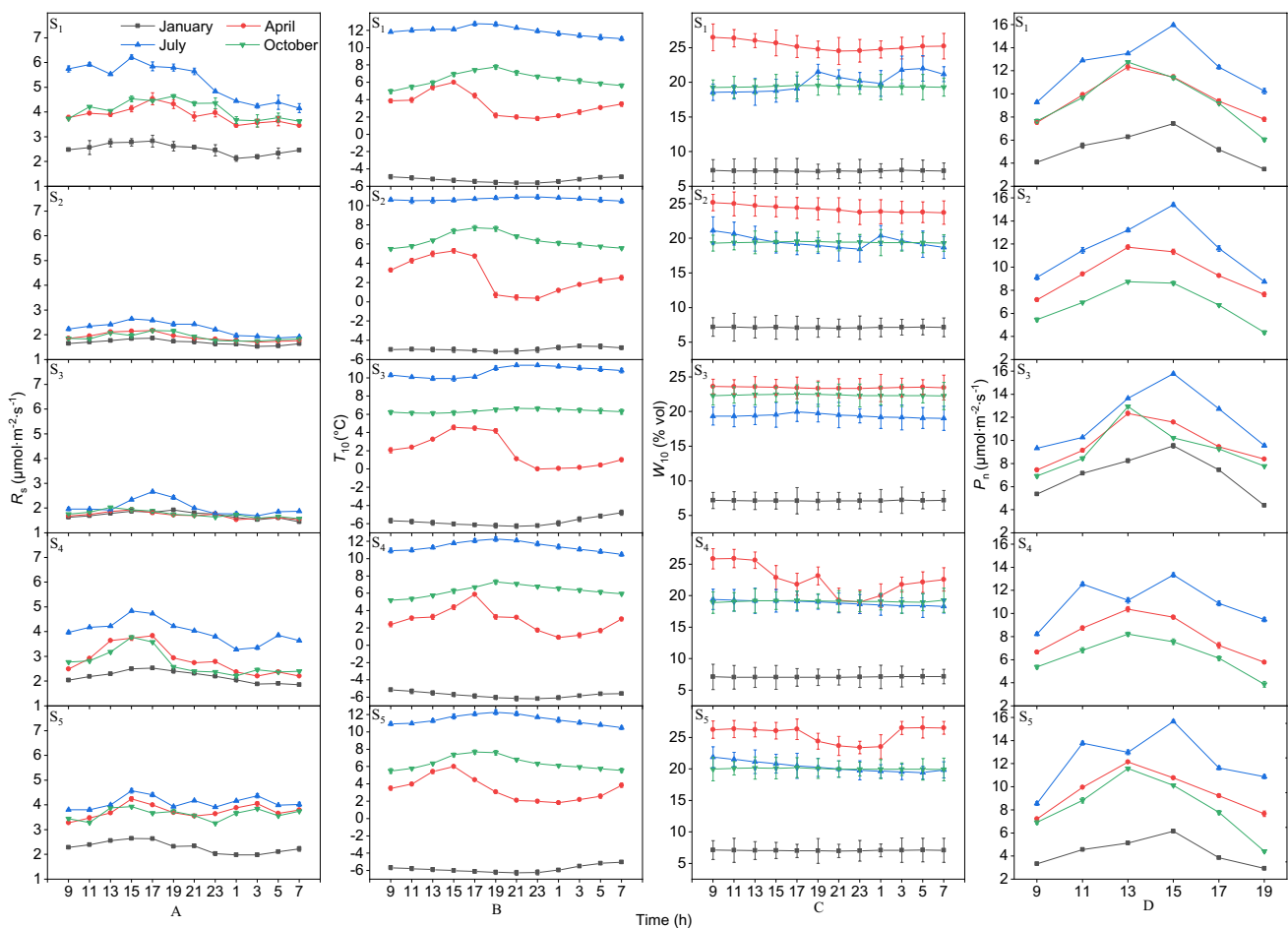


**Fig. 2** Diurnal variations in (A) soil respiration ( $R_s$ ), (B) soil temperature ( $T_{10}$ ) and (C) soil moisture content ( $W_{10}$ ) at 10 cm depth, and (D) net photosynthetic rate ( $P_n$ ) for different forest covers: Secondary

forest ( $S_1$ ), *L. principis-rupprechtii* ( $S_2$ ), *P. crassifolia* ( $S_3$ ), *P. cathayana* ( $S_4$ ), and *B. platyphylla* ( $S_5$ ) plantations in October 2018 and January, April, and July 2019. Vertical bars represented the means  $\pm$  SE



As shown in Fig. 2D, *P. cathayana* and *L. principis-rupprechtii* were not measured in the winter, because the leaves had fallen off completely. The diurnal variations in  $P_n$  in the ved species emerged as a bimodal type, which was different from the unimodal type of coniferous species. Furthermore, no remarkable diurnal variations in  $P_n$  were demonstrated with the five forest covers during the winter, and only those of  $S_1$  and  $S_3$  represented a significant change.

### Monthly variations in $R_s$ , $T_{10}$ , $W_{10}$ and $P_n$

As shown in Fig. 3, the trend of  $T_{10}$  decreased from September to January and then rebounded until August; with the lowest values in January. The temperature range in this area is large, and reaches  $-6.23$  to  $-0.94$  in January and  $12.07$ – $3.15$  in August. Overall, significant differences were not observed between the forest covers, except in January, July and August.

The  $W_{10}$  values were highest in April, fluctuated between May and August. During the spring and summer, the  $W_{10}$  values of forest covers represented extremely strong significance ( $p < 0.01$ ). The seasonal coefficients of variation (CV) were 40.59%, 40.09%, 39.23%, 34.41%, and 36.54%, respectively, which demonstrated severe fluctuations in the

water changes in the plantations of the five forest stands. In addition, the  $W_{10}$  of  $S_4$  was apparently lower than that of other forests during the growing season.

The trend of  $R_s$  changes with month was similar to that of  $T_{10}$ . The  $R_s$  readings of  $S_1$  were markedly higher than those of the other forest stands, while no significant difference was observed between  $S_2$  and  $S_3$ . During the nongrowing season (from October to March in the study site), the  $R_s$  values of *P. cathayana* plantations were dramatically lower than the others. The CV was 26.86%, 15.59%, 13.94%, 26.51%, and 21.94% for  $S_1$ – $S_5$ .

The variation regulation of  $P_n$  was similar to that of  $R_s$  throughout the year, except for the values in  $S_3$ , which were significantly higher than those of  $S_1$  and  $S_5$  during the winter. The  $P_n$  of  $S_4$  was significantly lower than that of the others, and no conspicuous difference was exhibited between  $S_1$  and  $S_5$ .

### Fitting relationship between the $R_s$ and the $T_{10}$ , $W_{10}$ and combination of $T_{10}$ and $W_{10}$

A significant exponential correlation was observed between  $R_s$  and  $T_{10}$  for the five forest covers ( $p < 0.05$ ). The highest  $R^2$  was observed in  $S_1$  (0.716), but it did not exceed 0.6 in

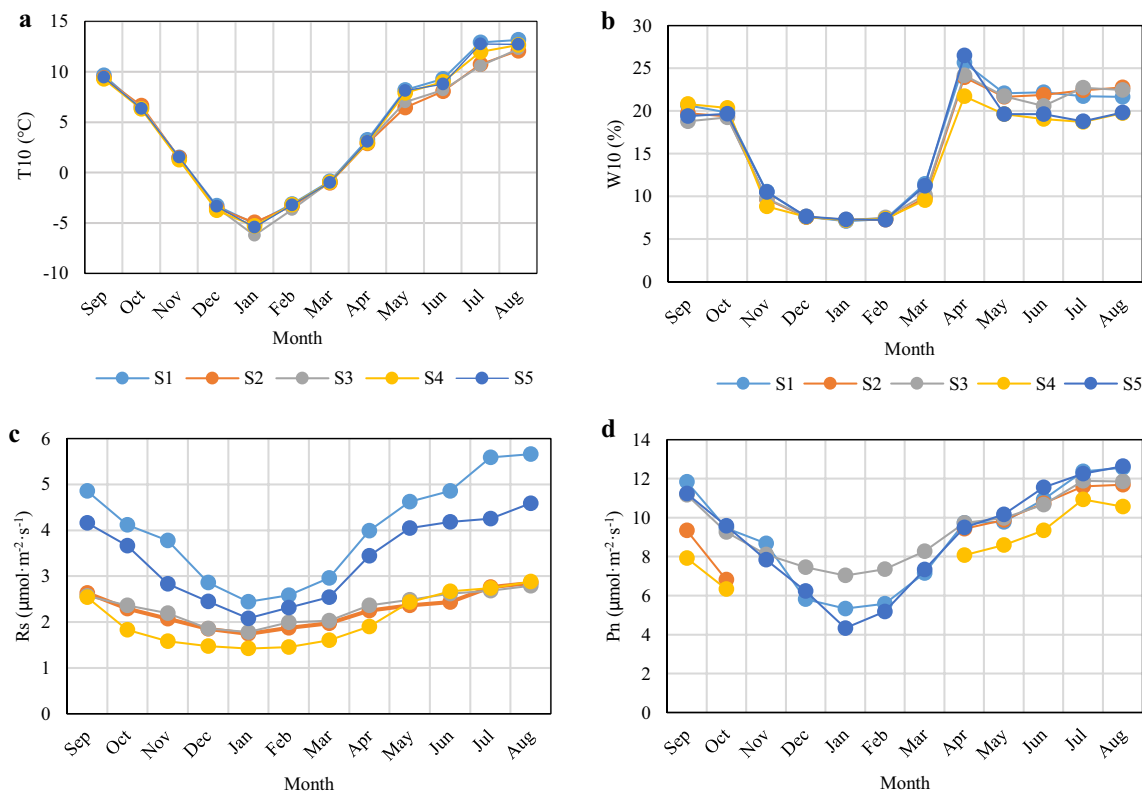


**Fig. 3** Monthly variations in soil temperature ( $T_{10}$ ) and (C) soil moisture content ( $W_{10}$ ) at 10 cm depth, soil respiration ( $R_s$ ), and net photosynthetic rate ( $P_n$ ) in different forest covers (Secondary forest

( $S_1$ ), *L. principis-rupprechtii* ( $S_2$ ), *P. crassifolia* ( $S_3$ ), *P. cathayana* ( $S_4$ ), and *B. platyphylla* ( $S_5$ ) plantations) from September 2018 to August 2019. Vertical bars represented the means  $\pm$  SE

the three other areas (Fig. 4).  $Q_{10}$  was highest in  $S_1$  and lowest in  $S_2$ . The  $Q_{10}$  value of broad-leaf forest was remarkably higher than that of coniferous forest (Table 3).

The goodness of fit for  $W_{10}$  was weaker, which was 35% less than the correlation between  $R_s$  and  $T_{10}$ . Furthermore, the fitted  $R_s$  model revealed remarkable effects of  $W_{10}$  on forest stands.

For the two-factor model with respect to  $T_{10}$  and  $W_{10}$ ,  $R^2$  was improved to different degrees in all forest covers, which explained 51.8% – 76.1% of the temporal variation in  $R_s$ .

**Response of  $R_s$  to other ecological factors**

$R_s$  had a positive correlation with all ecological factors (Fig. 5). However, significant correlations were not observed between  $R_s$  and the SOC, TK and soil C:N ratio ( $p > 0.05$ ). The correlation between  $R_s$  and  $P_n$  is shown in Fig. 6. Research has found that  $R_s$  increases with increasing  $P_n$  in various forest stands. Moreover, the slope of the relationship

was greater for measurements for  $S_1$  and  $S_5$ , while the lowest was revealed for  $S_2$ . Additionally,  $R^2$  value was lowest in  $S_4$  and highest in  $S_1$ .

**The relationship between  $R_s$  and the combination of  $T_{10}$ ,  $W_{10}$  and  $P_n$**

$T_{10}$ ,  $W_{10}$ ,  $P_n$  had significant effects on  $R_s$  (Figs. 4–6), and photosynthesis can provide the main supply of soil organic substrate for  $R_s$ .  $P_n$  was an important part of the assessment of  $R_s$  via the principal component analysis (mean variance contribution rate was 14.2%, not shown); thus, it was necessary to explore the combined effects of the three factors on  $R_s$ . Based on the model between  $R_s$  and the combination of  $T_{10}$  and  $W_{10}$  validated by predecessors, we further introduced  $P_n$  as a variable to establish the equation as follows:  $R_s = ae^{bT}W^cP_n^d$ , where  $a$ ,  $b$ ,  $c$  and  $d$  are undermined parameters. The model (Table 4) shows that the model fitting effect improved by introducing the  $P_n$  value was compared to the

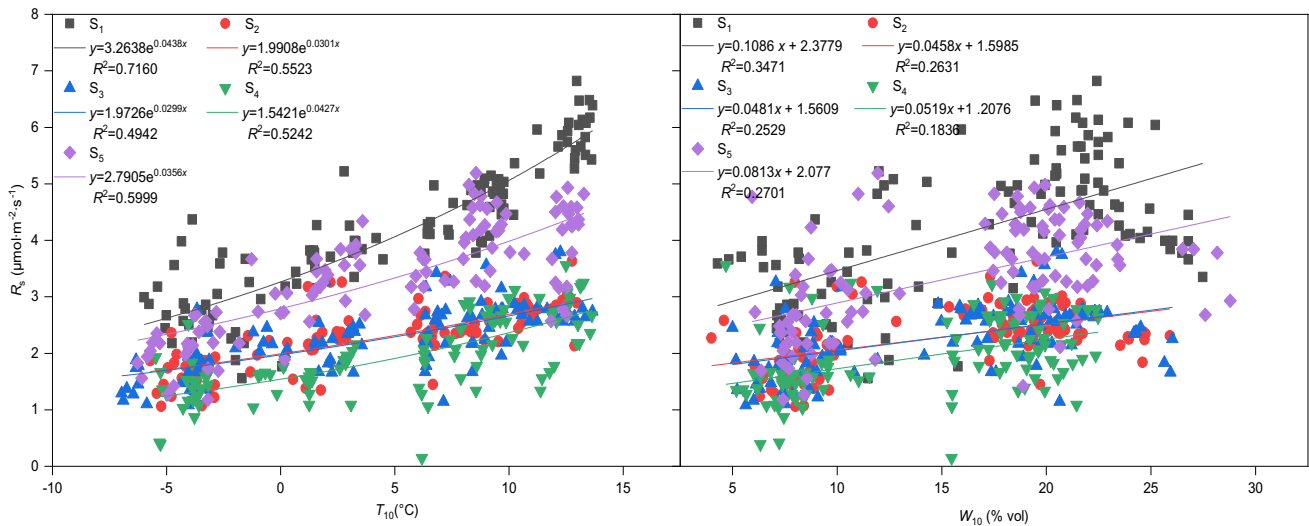


**Fig. 4** Exponential and linear fitting relationship between  $R_s$  and  $T_{10}$  and  $W_{10}$ , respectively.  $R^2$  represents the goodness of model fit after adjustment, the same as below.  $S_1$ ,  $S_2$ – $S_5$  refer to five representative

forest covers containing secondary forest ( $S_1$ ), *L. principis-rupprechtii* ( $S_2$ ), *P. crassifolia* ( $S_3$ ), *P. cathayana* ( $S_4$ ) and *B. platyphylla* ( $S_5$ ) plantations

**Table 3** Regression model parameters of  $R_s$  and  $T_{10}$ ,  $W_{10}$  and  $Q_{10}$

Forest covers	$R_s = ae^{bT}$			$R_s = aW + b$			$R_s = ae^{bT}W^c$				$Q_{10}$
	a	b	$R^2$	a	b	$R^2$	a	b	c	$R^2$	
$S_1$	3.264	0.0431	0.716**	0.109	2.378	0.347*	4.291	0.051	-0.012	0.761**	1.537a
$S_2$	1.991	0.0298	0.553*	0.046	1.599	0.263*	1.889	0.032	0.011	0.557*	1.349c
$S_3$	1.973	0.0300	0.494*	0.048	1.561	0.253*	2.022	0.034	-0.023	0.518*	1.352c
$S_4$	1.542	0.0427	0.424*	0.052	1.201	0.184*	1.685	0.046	-0.057	0.551*	1.535a
$S_5$	2.791	0.0352	0.600**	0.081	2.077	0.270*	2.292	0.038	0.059	0.632*	1.419b

Notes Significant correlations at  $*p < 0.05$  and  $**p < 0.01$ , respectively.  $S_1$ ,  $S_2$ – $S_5$  refer to five representative forest covers containing secondary forest ( $S_1$ ), *L. principis-rupprechtii* ( $S_2$ ), *P. crassifolia* ( $S_3$ ), *P. cathayana* ( $S_4$ ) and *B. platyphylla* ( $S_5$ ) plantations

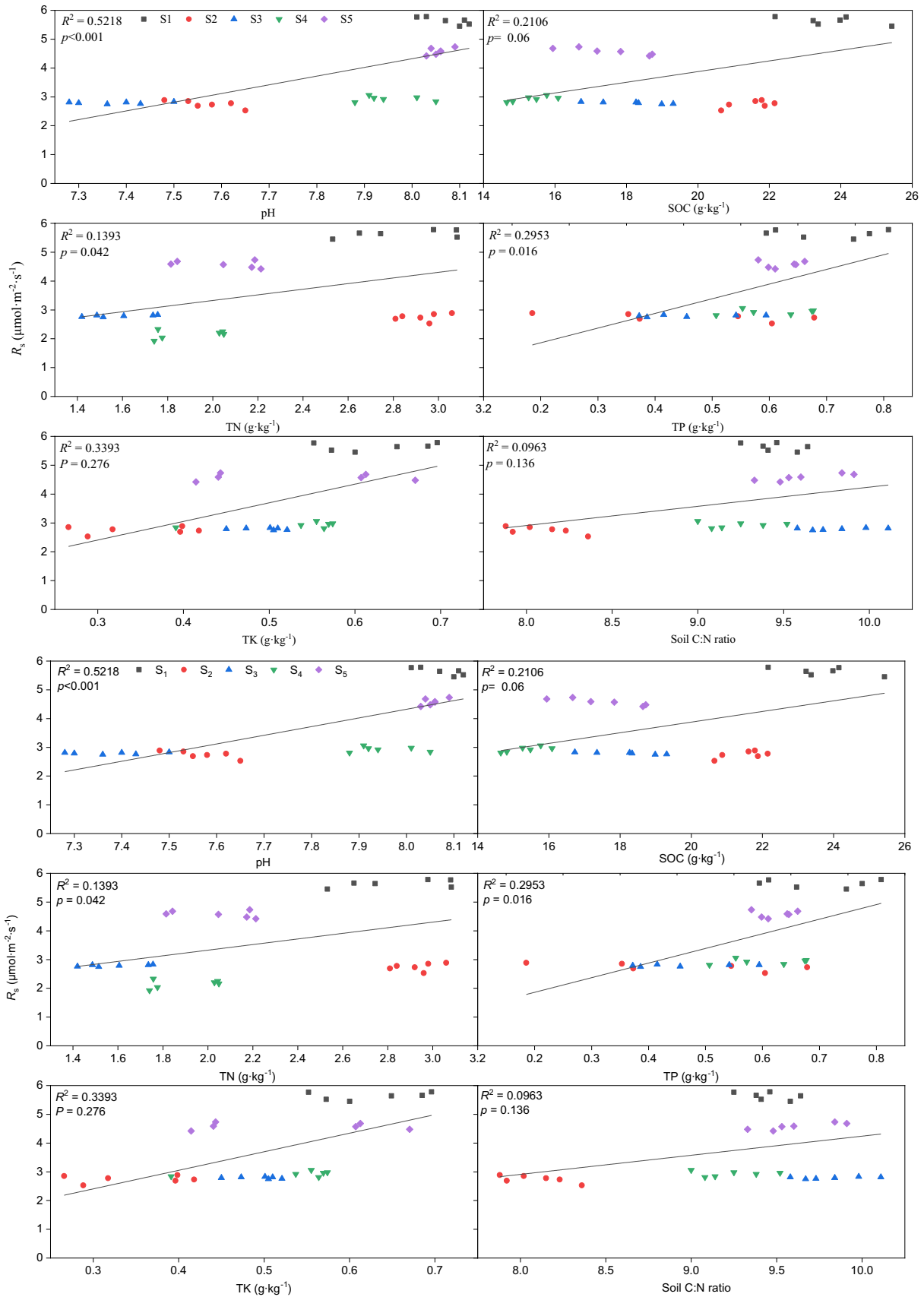




**Fig. 5** Linear relationship fitted between  $R_s$  and pH, SOC, TN, TP, TK and soil C:N ratio for all the forest covers ( $N=2$  measurements, a total of 6 replicates). All soil chemical indexes were assessed after the last  $R_s$  measurement date.

relationship between  $R_s$  and combination of the  $T_{10}$  and  $W_{10}$  (Table 3).

## Discussion

$T_s$  and soil water content (SWC) are the main environmental factors controlling  $R_s$ , and their changes will affect  $R_s$  in different stand types to different degrees. Limited diurnal variations occurred  $T_{10}$  and  $W_{10}$  in different forest covers because of the influence of closed canopies, and the result was different from the fluctuation of  $R_s$ , indicating that soil physical factors are not the main drivers of  $R_s$  dynamics at the diel scale. These phenomena were in line with findings in arid and semiarid regions (Jia et al. 2018). Furthermore, the  $R_s$  of the broad-leaved species was much higher than that of coniferous species during spring, summer, and autumn, which may be due to the increased alduronic acid secreted by the leaves of  $S_2$  and  $S_3$ , which caused soil acidification (refer to the pH value in Table 1) and slow decomposition of litter, thereby inhibiting the activity of microorganisms to reduce heterotrophic respiration. The  $R_s$  values in the daytime (photosynthesis was carried out synchronously) were greater than those at night, indicating that photosynthesis was coupled with respiratory mechanisms on a daily time scale. The seasonal variation trend of  $R_s$  was conspicuously regulated by  $T_{10}$  and  $W_{10}$ , in accordance with Chen's research on different subalpine ecosystems (Chen et al. 2014), and demonstrated the higher sensitivity of  $R_s$  to  $T_{10}$  and  $W_{10}$  on a seasonal scale compared to that on the daily scale. Moreover, photosynthetic productivity was an important driver of soil  $CO_2$  flux, not only on the daily time scale, but also on the seasonal and annual scales (Michael et al. 2008). In our study, the monthly variations in  $R_s$  and  $P_n$  maintained a high degree of consistency in different forest covers. Even in the winter when  $S_2$  and  $S_4$  lacked photosynthetic products, their  $R_s$  values simultaneously decreased to the minimum values. Our research also found that the  $R_s$  of  $S_1$  was significantly higher than that of pure forests throughout the year. By comparing the soil characteristics of each forest (Table 1), we found that the soil bulk density and the SOC, TN, TP and TK were significantly lower and higher than those of other forests, respectively. This result showed that the secondary forest structure (multilayer forest) was the most reasonable and could effectively alleviate intraspecies competition and promote plant growth and metabolism, thereby providing material conditions for carbon cycling.

$T_s$  contributes to regulating  $R_s$  by its effects on plant root growth, microbial activity, and litter decomposition; therefore, an exponential regression model was established for both (Song et al. 2013). Based on previous studies, we adjusted the parameters of the model to apply to the study area, then established a significant exponential model to demonstrate the regulatory effect of  $T_{10}$  on  $R_s$ , thereby providing theoretical support for the prediction of  $CO_2$  flux variations in alpine hilly areas under global warming. The correlation coefficient between  $R_s$  and  $T_{10}$  ranged from 49.4% in  $S_3$  to 71.6% in  $S_1$ . The reason for the difference may be due to the dissimilarity of the root systems and microbial activity (Chen et al. 2010), and even the regulation of photosynthesis by  $T_s$  ( $R^2=0.73$ ,  $p<0.05$ ) in plants may affect  $R_s$ . The correlation model of  $R_s$  and  $T$  can explain most of the seasonal and diel changes in soil C emissions, although the effect is not identical. Other factors such as soil moisture content affect  $R_s$  for a certain period of time. Therefore, we established a linear regression model of  $R_s$  and  $W_{10}$ . The correlation between  $R_s$  and SWC was significantly different in five forest types, which might be because the variation in  $W_{10}$  affected the input of carbon and the decomposition of litter and soil organic matter, thus indirectly affecting heterotrophic respiration and carbon output (Moyano et al. 2013). The correlation coefficients of the model were significantly lower than those based on  $R_s$  and  $T_{10}$ , which may have been caused by factors such as rainfall and severe evapotranspiration, and the related models established by SWC were not stable enough, as shown by the CV values (Fig. 3) for the forest types. In addition, sufficient precipitation occurred during study period, indicating that SWC was not a limiting factor for  $R_s$ .

Wang et al. (2006) believed that  $T_s$  is a great indicator for estimating  $R_s$  in a specific ecosystem, and verified the  $Q_{10}$  function to estimate the reliability of  $R_s$ , which is also confirmed by most ecosystems. The response of soil  $CO_2$  emission to  $T_s$  can be described by  $Q_{10}$  which is the  $T_s$  coefficient of the reaction (Ma et al. 2019). In this study, the  $Q_{10}$  value of broad-leaf forest was remarkably higher than that of coniferous forest, which was not in line with Zheng (Zheng et al. 2009), who found that the  $Q_{10}$  in deciduous forests was significantly higher than that in evergreen forests, and the  $Q_{10}$  in coniferous forests was significantly higher than that in evergreen broad-leaf forests. This difference may be because  $Q_{10}$  is not a long-term reflection of temperature sensitivity, but rather a comprehensive response to temperature fluctuations, root biomass and activity, humidity conditions, and other unknown variables (Janssens and Pilegaard 2003), thus resulting in indistinctness. Scholars have proposed that  $W_{10}$  thresholds exist in different forests. When  $W_{10}$  is higher than the threshold, the response of  $R_s$  to  $T_{10}$  may be confined by limiting aeration and  $CO_2$  diffusion, and

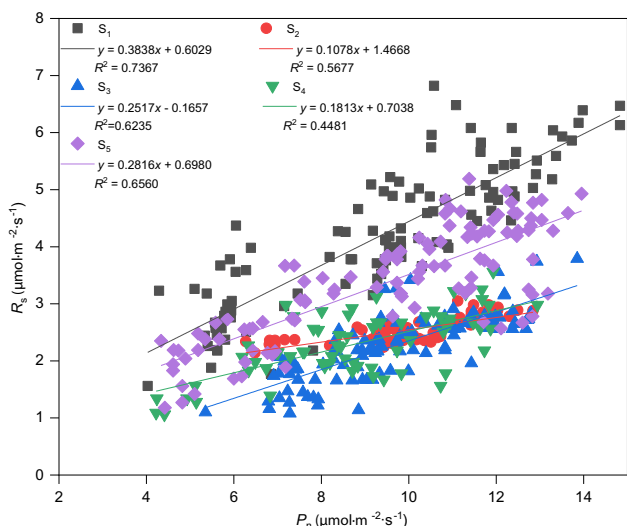


**Fig. 6** Linear fit of relationship between  $R_s$  and  $P_n$ , which is maintained at the same level of  $T_{10}$  and  $W_{10}$ .  $S_1$ ,  $S_2$ – $S_5$  refer to five representative forest covers containing secondary forest ( $S_1$ ), *L. principis-rupprechtii* ( $S_2$ ), *P. crassifolia* ( $S_3$ ), *P. cathayana* ( $S_4$ ) and *B. platyphylla* ( $S_5$ ) plantations

the decrease in soil microbial activity in a low oxygen environment may also lead to the reduction of soil CO<sub>2</sub> emissions, thereby restraining the sensitivity of  $R_s$  to  $T_{10}$  (Xu and Qi 2001b; Rey et al. 2002; Chen et al. 2010). Although  $T_{10}$  was not significantly different between the different forest stands, other ecological biological factors were significantly different, including SOC, TN, TP, TK, pH, soil bulk density and  $P_n$ . Moreover,  $Q_{10}$  was highest in  $S_1$  because it belonged to the enclosed forest protected from human activities, and  $S_1$  was characterized by a sufficient supply of soil organic substrate, higher root biomass, and microbial activity, and more complex and stable species composition compared to other forests. However, this result also implied that the carbon cycle might experience a greater disturbance under global warming. Therefore, the process of global warming and carbon cycle promote and influence each other and are complementary.

The combination of  $T_s$  and SWC on  $R_s$  is critical to understanding the mechanisms of climate control on  $R_s$  and its components (Ma et al. 2019). The response of  $R_s$  to  $T_{10}$  and  $W_{10}$  in this study area has been proven, and it is worth exploring whether there is an interactive or complementary effect of  $T_{10}$  and  $W_{10}$  on  $R_s$ . We established a two-factor model combining  $W_{10}$  and  $T_{10}$  compared to the model-based only on  $T_{10}$  or  $W_{10}$ , which improved  $R^2$  to different degrees, this circumstance has been ascertained by others research (Zhang et al. 2010; Gao et al. 2018; Ma et al. 2019). According to our results, the variation trend of  $R_s$  increased with the escalation of  $W_{10}$  and  $T_{10}$ . From May to August, when  $W_{10}$  remained basically stable, the increase in  $T_{10}$  promoted the increase in  $R_s$  by boosting the root system and microbial activity.

When exploring the response of  $R_s$  to other ecological environmental factors, we observed that the variation in  $R_s$  was not in conformity with that of SOC, TK and the soil C:N ratio, which was also confirmed by Gao et al. (2018) in a study of the correlation between  $R_s$  and environmental factors. In addition,  $R_s$  was weakly consistently correlated with TN and TP (Nielsen and Becky 2015; Wertin et al. 2018). The findings indicated that the combined indicators rather than a single factor regulate the changes of  $R_s$ , which complicates the evaluation of  $R_s$  (Okin et al. 2016). Soil properties can be influenced by forest types and act on soil microbial and root activity (Lu et al. 2014). Our research found that  $R_s$  can be significantly affected by pH, which is further evidence that coniferous forest leaves contribute to soil acidification, thus reducing  $R_s$ .

Previous research revealed that  $T_{10}$  and  $W_{10}$  together could explain more than 75% of the variation in  $R_s$  (Keith et al. 1997). Since the components that affect changes in  $R_s$  are not completely clear, we are particularly interested in the contribution of  $P_n$  to  $R_s$  with species of contrasting functional types. We analyzed the correlation between the  $P_n$  value and  $R_s$  of each forest cover type and found that  $P_n$  was significantly positively correlated with  $R_s$ , which is consistent with studies showing the close coupling of *A. hymenoides* and *A. confertifolia* leaf-level  $P_n$  and  $R_s$  (Wertin

**Table 4** The regression model parameters for  $R_s = ae^{bT}W^cP_n^d$ . The equation is established according to the synchronous measurement data of each index

Forest cover	Regression model parameters values					
	<i>a</i>	<i>b</i>	<i>c</i>	<i>d</i>	<i>R</i> <sup>2</sup>	<i>p</i>
$S_1$	2.0458	0.0331	−0.1192	0.3811	0.7860	0.0222
$S_2$	1.4052	0.0132	−0.0282	0.2511	0.6221	0.0037
$S_3$	0.1702	−1.8370	0.0101	1.1232	0.6305	0.0292
$S_4$	0.8291	0.0131	−0.1547	0.6122	0.5710	0.0324
$S_5$	0.9394	−0.6248	−0.0010	0.8973	0.6971	0.0325

Notes  $S_1$ ,  $S_2$ – $S_5$  refer to five representative forest covers containing secondary forest ( $S_1$ ), *L. principis-rupprechtii* ( $S_2$ ), *P. crassifolia* ( $S_3$ ), *P. cathayana* ( $S_4$ ) and *B. platyphylla* ( $S_5$ ) plantations. (*b* is the parameter that needs to be corrected in the formula; *T* is the temperature)

et al. 2017, 2018). Other studies have demonstrated the close correlation between  $P_n$  and  $R_s$  in dryland ecosystems (Chen et al. 2009). This result showed that the photosynthetic C supply acted as a driving factor for  $R_s$  and  $P_n$ , and regulated  $R_s$  by stimulating root respiration and heterotrophic respiration of root deposition. Moreover, studies have also suggested a more compact coupling between photosynthetic products and  $R_s$  than between  $R_s$  and other factors (Vargas et al.; 2010a, b; Jia et al. 2018). We can also support this result by analyzing the correlation between the  $P_n$  of a single-leaf horizontal and  $R_s$ ;  $R^2$  was higher than that of the model based only on  $W_{10}$  and  $T_{10}$ . Furthermore, the  $R^2$  between  $P_n$  and  $R_s$  was lowest in  $S_4$  and highest in  $S_1$ . We speculated that  $S_1$  was located in the fenced-in zone, which was not disturbed by human activity, and that production and behaviors would introduce more substrate and change the mechanisms underlying underground C supply, thereby reducing the effect of photosynthesis on  $R_s$ . But why is the correlation coefficient lowest in  $S_4$  if it is an artificial forest subjected to more human disturbance? The daily change in  $P_n$  is bimodal with solar radiation, temperature, and humidity in most of the observation periods, and the severe water consumption characteristics of *P. cathayana* reduced the biomass and microbial activity of the forest. In addition, the high incidence of black spot disease in August severely inhibited leaf photosynthesis during period of growth and metabolism, as shown in Fig. 3. Therefore, to more comprehensively evaluate the main factors controlling  $R_s$  in different forest ecosystems in subalpine hilly areas, we introduced  $P_n$  to establish a three-factor model. The results exhibited a significant improvement in the fitting correlation coefficient compared to that of the two-factor model based on the combination of  $T_{10}$  and  $W_{10}$ . Our results suggest that the control of  $R_s$  by the environment (moisture and temperature) and photosynthesis may be spatially and temporally homeostatic in the region; thus, the model was feasible for describing the dynamic variation in the  $R_s$  and the carbon cycle under different forest covers.

However, the pattern of underground C supply and distribution is not yet clear. Although these findings help fill some gaps in knowledge of  $R_s$  dynamics in different forest ecosystems under current climatic conditions, further research should focus on the driving factors of autotrophic respiration and heterotrophic respiration, and the response of microorganisms to climate change needs to be explored.

## Conclusion

During spring, summer, and autumn, the diurnal variations in  $R_s$  were significantly greater in the afternoon than at other times, and the  $R_s$  was pronouncedly higher for broad-leaved species than for coniferous species in the five typical forest

covers. Our study also found that  $R_s$  could be significantly affected by soil pH, which provided further evidence that coniferous forest leaves contribute to soil acidification, thus reducing  $R_s$ . Furthermore, soil physical factors are not the main drivers of  $R_s$  dynamics at the diel scale; however, the trend in the monthly variation trend of  $R_s$  was consistent with that of  $T_{10}$  and  $P_n$ . The  $R_s$  of  $S_1$  was significantly higher than the value found in pure forests throughout the year.

The  $R^2$  for the model based on  $R_s$  and  $T_{10}$  was significantly higher than for the model based on  $R_s$  and  $W_{10}$ . Moreover, the two-factor model that combined  $T_{10}$  and  $W_{10}$  with adjusted parameters improved the  $R^2$  value at a different level compared with the model based only on  $T_{10}$  and  $W_{10}$ , indicating that the  $R_s$  was influenced by the combined effect of  $T_{10}$  and  $W_{10}$ , which was interactive or complementary in different forest ecosystems in the alpine hilly region. The  $Q_{10}$  value for the broad-leaved forest was remarkably higher than for the coniferous forest, and the highest value was discovered in the secondary forest. Our findings showed that a combination of soil chemical properties rather than a single factor may regulate the changes of  $R_s$ , which complicates the evaluation of  $R_s$ .

By evaluating the correlation between the  $P_n$  at the single-leaf level and  $R_s$ , we proved that  $P_n$  was closely coupled with  $R_s$  in all the measured forests. Furthermore, the  $R^2$  between  $P_n$  and  $R_s$  was lowest in *Populus cathayana* plantations and highest in the secondary forest. The results showed that the three-factor model presented significant improvements in  $R^2$  compared to the two-factor model based on the combination of  $T_{10}$  and  $W_{10}$  and thus is, feasible for describing the dynamic variation in  $R_s$ .

## References

- Ardö J, Olsson L (2003) Assessment of soil organic carbon in semi-arid Sudan using GIS and the CENTURY model. *Arid Environ* 54(4):633–651
- Chen SP, Lin GH, Huang JH, Jenerette GD (2009) Dependence of carbon sequestration on the differential responses of ecosystem photosynthesis and respiration to rain pulses in a semiarid steppe. *Glob Change Biol* 15(10):2450–2461
- Chen BY, Liu SR, Ge JP, Chu JX (2010) Annual and seasonal variations of  $Q_{10}$  soil respiration in the sub-alpine forests of the Eastern Qinghai-Tibet Plateau. *China Soil Bio Biochem* 42(10):1735–1742
- Chen YC, Luo J, Li W, Yu D, She J (2014) Comparison of soil respiration among three different subalpine ecosystems on eastern Tibetan Plateau. *China Soil Sci Plant Nutr* 60(2):231–241
- ChenST WJ, Zhang TT, Hu Z (2020) Climatic, soil, and vegetation controls of the temperature sensitivity ( $Q_{10}$ ) of soil respiration across terrestrial biomes. *Glob Ecol Conserv* 22:e00955
- Chesney M, Lasserre P, Troja B (2017) Mitigating global warming: a real options approach. *Ann Oper Res* 255:465–506
- Clark MS, Horwath WR, Shennan C (1998) Changes in soil chemical properties resulting from organic and low-input farming practices. *Agron J* 90(5):662–671

- Crowther WT, Bradford MA, Johnson N (2013) Thermal acclimation in widespread heterotrophic soil microbes. *Ecol Lett* 16(4):469–477
- Curiel Yuste J, Janssens IA, Carrar A, Ceulemans R (2010) Annual Q10 of soil respiration reflects plant phenological patterns as well as temperature sensitivity [J]. *Glob Change Biol* 10(2):161–169. <https://doi.org/10.1111/j.1529-8817.2003.00727.x>
- Feng YZ, Grogan P, Caporaso JG, Zhang H, Lin XG, Knight R, Chu HY (2014) pH is a good predictor of the distribution of anoxygenic purple phototrophic bacteria in Arctic soils. *Soil Biol Biochem* 74(6):193–200
- Flanagan LB, Johnson BG (2005) Interacting effects of temperature, soil moisture and plant biomass production on ecosystem respiration in a northern temperate grassland. *Agric For Meteorol* 130(3):237–253
- Friedlingstein P, Andrew RM, Rogelj J, Peters GP, Canadell JG, Knutti R, Luderer G, Raupach MR, Schaeffer M, Vuuren DP (2014) Persistent growth of CO<sub>2</sub> emissions and implications for reaching climate targets. *Nat Geosci* 7(10):709–715
- Fu Q, Johanson CM, Wallace JM, Reichler T (2006) Enhanced mid-latitude tropospheric warming in satellite measurements. *Science* 312(5777):1179
- Gao W, Huang ZQ, Ye GF, Yue XJ, Chen ZY (2018) Effects of forest cover types and environmental factors on soil respiration dynamics in a coastal sand dune of subtropical China. *J For Res* 29(6):1645–1655
- Hanson PJ, Edwards NT, Garten CT, Andrews JA, Rustad LE, Huntington TG, Boone RD (2000) Separating root and soil microbial contributions to soil respiration: A review of methods and observations. *Biogeochemistry* 48(1):115–146
- Hashimoto S (2012) A new estimation of global soil greenhouse gas fluxes using a simple data-oriented model. *PLoS ONE* 7(8):e41962
- Heinemeyer A, Wilkinson M, Vargas R, Subke JA, Casella E, Morison JJ, Ineson P (2012) Exploring the Boverflow tap theory: linking forest soil CO<sub>2</sub> fluxes and individual mycorrhizosphere components to photosynthesis. *Biogeosciences* 9(1):79–95
- Hölttä MT (2010) The significance of phloem transport for the speed with which canopy photosynthesis and belowground respiration are linked. *New Phytol* 185(1):189–203
- Janssens IA, Pilegaard KIM (2003) Large seasonal changes in Q10 of soil respiration in a beech forest. *Glob Change Biol* 9(6):911–918
- Jia X, Zha T, Wang S, Bourque PA, Wang B, Qin S, Zhang Y (2018) Canopy photosynthesis modulates soil respiration in a temperate semi-arid shrubland at multiple timescales. *Plant Soil* 432:437–450
- Keith H, Jacobsen KL, Raison RJ (1997) Effects of soil phosphorus availability, temperature and moisture on soil respiration in *Eucalyptus pauciflora* forest. *Plant Soil* 190(1):127–141
- Lal R (2008) Sequestration of atmospheric CO<sub>2</sub> in global carbon pools. *Energy Environ Sci* 1(1):86–100
- Landesman WJ, Nelson DM, Fitzpatrick MC (2014) Soil properties and tree species drive  $\beta$ -diversity of soil bacterial communities. *Soil Biol Biochem* 76:201–209
- Li GY, Mu JP, Liu YZ, Sun S (2017) Effect of microtopography on soil respiration in an alpine meadow of the Qinghai-Tibetan plateau. *Plant Soil* 421(1–2):147–155
- Liu X, Chen B (2000) Climatic warming in the Tibetan Plateau during recent decades. *Int J Climatol* 20(14):1729–1742
- Lu XQ, Toda H, Ding FJ, Fang SZ, Yang WX, Xu HG (2014) Effect of vegetation types on chemical and biological properties of soils of karst ecosystems. *Eur J Soil Biol* 61(3):49–57
- Ma MZ, Zang ZH, Xie ZQ, Chen QS, Xu WT, Zhao CM, Shen GZ (2019) Soil respiration of four forests along elevation gradient in northern subtropical China. *Ecol Evol* 9(22):12846–12857
- Michael B, Rodeghiero M, Anderson-Dunn M, Dore S, Gimeno S, Drösler M, Williams M, Ammann C, Berninger F, Flechard C (2008) Soil respiration in European grasslands in relation to climate and assimilate supply. *Ecosystems* 11(8):1352–1367
- Mitchell RJ, Marrs RH, Le MGD (1999) A study of the restoration of heathland on successional sites: changes in vegetation and soil chemical properties. *J Appl Ecol* 36(5):770–783
- Moyano FE, Stefano M, Claire C (2013) Responses of soil heterotrophic respiration to moisture availability: an exploration of processes and models. *Soil Biol Biochem* 59:72–85
- Nielsen UN, Becky AB (2015) Impacts of altered precipitation regimes on soil communities and biogeochemistry in arid and semi-arid ecosystems. *Glob Change Biol* 21(4):1407–1421
- Okin GS, Moreno DLH, Patricia MS, Throop L, Enrique RV, Anthony JP, Wainwright J, Debra PFP (2016) Connectivity in dryland landscapes: shifting concepts of spatial interactions. *Heather Ecol Environ* 13(1):20–27
- Peng F, Xue X YQG, Tao W (2015) Warming effects on carbon release in a permafrost area of Qinghai-Tibet Plateau. *Environ Earth Sci* 73(1):57–66
- Raich JW, Potter CS, Bhagawati D (2002) Bhagawati interannual variability in global soil respiration. *Glob Change Biol* 8(8):800–812
- Ren F, Yang XX, Zhou HK, Chen L, Cao G, He JS (2017) Corrigendum: Contrasting effects of nitrogen and phosphorus addition on soil respiration in an alpine grassland on the Qinghai-Tibetan Plateau. *Sci Rep* 7(7):39895
- Rey A, Pegoraro E, Tedeschi V, Parri ID, Jarvis PG, Valentini R (2002) Annual variation in soil respiration and its components in a coppice oak forest in Central Italy. *Glob Change Biol* 8(9):851–866
- Sheng H, Yang YS, Yang ZJ, Chen GS, Xie JS, Guo JF, Zou SQ (2010) The dynamic response of soil respiration to land-use changes in subtropical China. *Glob Change Biol* 16(3):1107–1121
- Song XZ, Yuan HY, Kimberley MO, Jiang H, Zhou GM, Wang HL (2013) Soil CO<sub>2</sub> flux dynamics in the two main plantation forest types in subtropical China. *Sci Total Environ* 444:363–368
- Udelhoven T, Emmerling C, Jarmer T (2003) Quantitative analysis of soil chemical properties with diffuse reflectance spectrometry and partial least-square regression: a feasibility study. *Plant Soil* 251(2):319–329
- Vargas R, Baldocchi DD, Allen MF, Bahn M, Black TA, Collins SL, Yuste JC, Hirano T, Jassal RS, Pumpanen J (2010a) Looking deeper into the soil: biophysical controls and seasonal lags of soil CO<sub>2</sub> production and efflux. *Ecol Appl* 20(6):1569–1582
- Vargas R, Baldocchi DD, Allen MF, Bahn M, Black TA, Collins SL, Yuste JC, Hirano T, Jassal RS, Pumpanen J, Tang JW (2010b) Looking deeper into the soil: biophysical controls and seasonal lags of soil CO<sub>2</sub> production and efflux. *Ecol Appl A Pub Ecol Soc Am* 20(6):1569–1582
- Wang CK, Yang JY, Zhang QZ (2006) Soil respiration in six temperate forests in China. *Glob Change Biol* 12(11):2103–2114
- Wertin TM, Belnap J, Reed SC (2017) Experimental warming in a dryland community reduced plant photosynthesis and soil CO<sub>2</sub> efflux although the relationship between the fluxes remained unchanged. *Funct Ecol* 31(2):297–305
- Wertin TM, Young K, Sasha CR (2018) Spatially explicit patterns in a dryland's soil respiration and relationships with climate, whole plant photosynthesis and soil fertility. *Oikos* 127(9):1280–1290
- West CPA, Mallarino P, Wedin WF (1989) Spatial variability of soil chemical properties in grazed pastures. *Soil Sci Soc Am J* 53(3):784–789
- White I (1988) Measurement of soil physical properties in the field. In Steffen WL, Denmead OT (eds) *Flow and transport in the natural environment: advances and applications*. Springer Berlin Heidelberg, Berlin, pp 59–85
- Wu X, Xu H, Tu DF, Liu GH (2020) Land use change and stand age regulate soil respiration by influencing soil substrate supply and microbial community. *Geoderma* 359:113991

- Xu M, Qi Y (2001a) Soil-surface CO<sub>2</sub> efflux and its spatial and temporal variations in a young ponderosa pine plantation in northern California. *Glob Change Biol* 7(6):667–677
- Xu M, Qi Y (2001b) Spatial and seasonal variations of Q<sub>10</sub> determined by soil respiration measurements at a Sierra Nevada forest. *Global Biogeochem Cycles* 15(3):687–696
- Xu Z, Yin H, Zhao C (2018) Responses of soil respiration to warming vary between growing season and non-growing season in a mountain forest of southwestern China. *Can J Soil Sci* 98(1):70–76
- Yao YZ, Wang YR, Li YH, Liu B (2005) The warming and drying of the loess plateau in China and its impact on the ecological environment. *Resources Science (In Chinese)* 5:67–75
- Zeng X, Zhang W, Shen H, Xin Z (2014) Soil respiration response in different vegetation types at Mount Taihang China. *CATENA* 116(5):78–85
- Zhang LH, Chen YN, Zhao RF, Li WH (2010) Significance of temperature and soil water content on soil respiration in three desert ecosystems in Northwest China. *J Arid Environ* 74(10):1200–1211
- Zheng ZM, Yu GR, Fu YL, Wang YS, Sun XM, Wang YH (2009) Temperature sensitivity of soil respiration is affected by prevailing climatic conditions and soil organic carbon content: a trans-China based case study. *Soil Biol Biochem* 41(7):1531–1540
- Zhou T, Ren L, Liu H, Lu J (2018) Impact of 1.5 °C and 2.0 °C global warming on aircraft takeoff performance in China. *Sci Bull* 63(11):700–707

**Publisher's Note** Springer Nature remains neutral with regard to jurisdictional claims in published maps and institutional affiliations.